NO_x Depolluting Performance of Photocatalytic Materials in an Urban Area - Part II: Assessment through Computational Fluid Dynamics Simulations

Beatriz Sanchez[a,b,*], Jose Luis Santiago[b], Alberto Martilli[b], Magdalena Palacios[b], Lourdes Núñez[b], Manuel Pujadas[b], Jaime Fernández-Pampillón[b,c]

[a] *Department of Geography, National University of Singapore, Singapore*

[b] *Research Center for Energy, Environment and Technology (CIEMAT), Madrid, Spain*

[c] *The National Distance Education University (UNED), Madrid, Spain*

Abstract

Photocatalytic materials are proposed as a mitigation strategy of urban air pollution because of its deposition feature. This study aims at evaluating their effect on NO_2 concentrations in an urban environment under real atmospheric conditions through Computational Fluid Dynamics (CFD) simulations. A comprehensive study is performed to determine the potential of photocatalytic materials to remove NO_2 at pedestrian level taking into account the variability of wind speed, traffic emissions and the photoactive area in an urban environment. The deposition velocity used to model the sink effect of a photoactive surface is derived from laboratory data and its applicability to outdoor conditions is proved through microscale simulations. The CFD simulation performed to assess the impact of a photocatalytic material on ambient pollutants in a real urban scenario is evaluated against the measurements presented in Part I (Fernández-Pampillón et al., 2020). Results show that the application of photocatalytic materials in an urban environment yield a minimal reduction in NO_2 concentrations below 1% under the studied atmospheric conditions. In a hypothetical scenario, in which the photoactive area is extended to an entire neighbourhood, small decrease of NO_2 concentrations below 2% is obtained under the daytime prevailing atmospheric conditions of the area of interest. Finally, the reduction of NO_2 under several atmospheric conditions results to be mainly dominated by wind flow and NO_x emissions in the study street.

Keywords: CFD model, NO_2 Mitigation Strategies, NO_x-O_3 chemistry, Photocatalytic materials, Urban Air Quality

*Corresponding author.
Email address: geobss@nus.edu.sg (Beatriz Sanchez)

1. Introduction

Air pollution is still an important concern in urban environments, and air quality management become a priority challenge in many cities nowadays. High levels of NO_x are mostly dominated by its main source in urban areas, road traffic (EEA, 2015). In particular, NO_2 is under consideration because of its adverse effects both in short- and long-term on human health (WHO, 2013). Hence mitigation strategies are needed to reduce population exposure to NO_2 levels and thus to improve urban air quality.

Photocatalytic materials emerge as a technology for air purification that can be used for air pollution abatement. Titanium dioxide (TiO_2) is an excellent photocatalyst that is activated in presence of sunlight and lead to the decomposition of molecules adsorbed on the photoactive surface (Schneider et al., 2014). Many pollutants can be decomposed by ultraviolet (UV) radiation, however TiO_2 can accelerate the removal of nitrogen oxides (NO_x), sulfur oxides (SO_x) and volatile organic compounds (VOC) by trapping and degrading them from air in presence of sunlight (Hassan et al., 2012).

Testing efficiency of photocatalytic materials to reduce NO_x levels is widely analysed in a flow reactor (Zouzelka and Rathousky, 2017; Jõgi et al., 2016; Ballari et al., 2010; Hüsken et al., 2009). In standard laboratory tests, the relation between the irradiated photocatalytic surface and volume of air is 1:5 ($\cdot 10^3$ m^{-1}) (ISO 22197-1:2007), which determines the probability of molecules to interact with the photoactive surface. However, the percentage reduction from these materials, obtained in laboratory conditions, cannot be directly extrapolated to the urban atmosphere in order to obtain the impact of photocatalytic materials on pollutant levels in urban environments. It is mainly due to the fact that the relation between the treated surface and volume of air is not comparable, and besides, the environmental conditions (irregular urban morphology or heterogeneity of traffic emissions) and the complexity of dynamics, chemical and turbulent processes significantly differ from laboratory conditions. Consequently, all these factors modify the NO_2 abatement caused by the photocatalytic materials in urban environments.

For the foregoing reasons, some recent studies addressed the assessment of photocatalytic materials during thorough field campaigns in outdoor conditions (Fernández-Pampillón et al., 2020; Cordero et al., 2020; Gallus et al., 2015a,b; Ballari and Brouwers, 2013; Guerrini, 2012; Chen and Chu, 2011; Maggos et al., 2008). Fernández-Pampillón et al. (2020) evaluated the impact on ambient NO_x in an urban area after applying a photocatalytic material on the road. Several sampling points were deployed along the street to record NO_x concentrations during months. The complexity of atmospheric processes and urban factors revealed the difficulty to quantify the impact of photocatalytic materials on ambient NO_x concentrations through measurements taken in a real urban environment. Gallus et al. (2015a) carried out an exhaustive field campaign in a road tunnel assessing the NO_x removal under different approaches. Despite the results obtained in laboratory, no significant reduction in NO_x was found in the tunnel. In addition, they observed an important decrease in the photocatalytic activity under heavily polluted conditions.

Modelling the dispersion of reactive pollutants (e.g. NO_2) in urban environments is still a big challenge using Computational Fluid Dynamics (CFD) models. Several numerical studies have implemented chemical mechanisms to simulate the NO_2 dispersion in simplified street canyons (Zhong et al., 2016; Sanchez et al., 2016; Zhong et al., 2017). However, just a few incorporated chemical reactions to examine the NO_2 transport in irregular geometries (Kwak et al., 2015; Santiago et al., 2017). Through CFD models, air pollution dispersion in urban environments are commonly addressed considering non-reactive pollutants (Amorim et al., 2013; Sanchez et al., 2017; Kwak et al., 2018; Rivas et al., 2019; Santiago et al., 2020). To our knowledge, there are barely studies evaluating the impact of photocatalytic materials on air pollution in real urban areas using CFD models. The NO_x removal due to the interaction of ambient pollutants with the photoactive surface can be simulated through an effective deposition rate. Same approach is commonly applied to model the deposition process on the leaves of the urban vegetation (Buccolieri et al., 2018). Jeanjean et al. (2017) performed a comparative study of mitigation measures for NO_2 levels in a street from the environment and economic perspective using CFD simulations. NO_2 reduction due to photocatalytic materials was modelled assuming a deposition velocity for NO_2, without considering atmospheric chemistry. The photocatalytic paint coated facades on each side of the street (30 000 m^2) provided average reductions of NO_2 ranging between 0.6% and 1.2%. The impact of photoactive building walls on overall air quality resulted to be small in addition to be more expensive than other alternative strategies.

Hence the following research questions arise: 1) *How effective is the extensive use of photocatalytic material to reduce NO_2 concentration in a real urban environment?* and 2) *How sensitive is this reduction to variations of meteorological conditions (e.g. wind speed) or urban factors (e.g. traffic intensity)?*

Through CFD simulations, this work attempts to investigate the NO_2 mitigation at pedestrian height by applying photocatalytic materials in an urban area. In this study, the modelling approach consists of implementing a deposition rate for NO on the photoactive surface and the subsequent effect on NO_2 is tackled by modelling atmospheric chemical reactions. The effect of a photoactive area in a street to reduce the NO_2 pollution levels is examined and compared against measurements presented in Part I (Fernández-Pampillón et al., 2020). Additionally, a broader study is performed to assess the influence on the NO_2 reduction caused by the variability of wind speed and traffic emissions in an urban environment. Numerical outcomes from this study are evaluated with observations from field campaigns performed at each urban setting within the framework of the LIFE MINOx−STREET European Project (LIFE12 ENV/ES/000280).

2. CFD-RANS model description

The CFD model used is based on the Reynolds−averaged Navier−Stokes (RANS) equations with the Realizable $k-\varepsilon$ turbulence closure (STARCCM+ from Siemens). This approach has been successfully applied to real urban environments (Santiago et al., 2017; Sanchez et al., 2017). In urban environments, the proximity between sources and receptors and fast

turbulent processes in the street entails that just chemical reactions with a short timescale have a significant impact on modelled NO_2 concentrations at pedestrian level (Sanchez et al., 2016). At daytime, the interconversion of NO, NO_2 and O_3 is generally dominated by the photostationary chemical mechanism (Leighton relationship (Clapp and Jenkin, 2001)).

$$NO_2 + h\nu \longrightarrow NO + O \quad (1)$$

$$O + O_2 + M \longrightarrow O_3 + M \quad (2)$$

$$O_3 + NO \longrightarrow NO_2 + O_2 \quad (3)$$

M denotes a molecule that absorbs excess energy and thereby stabilizes the O_3 molecule formed. The highly reactive oxygen atom (O) allows to assume that the formation rate of O by Reaction (1) is the same as the depletion rate of O by Reaction (2) based on the pseudo-steady-state approximation (Seinfeld and Pandis, 1998). In the photochemical Reaction (1), the photolysis rate constant (J_{NO_2}) depends on zenith angle (θ) as $J_{NO_2} = A \cdot exp(B/cos(\theta))$, where A and B are chemical constants. The rate constant (k) for the Reaction (3) is defined as function of air temperature ($k = A \cdot exp(-B/T)$). Both variables, θ and air temperature vary as a function of the simulated hour. Therefore, dispersion of NO, NO_2 and O_3 is modelled through the 3 transport equations for each pollutant involving the chemical terms that appear in the chemical mechanism. The time step is set at 1 s both for the dynamical and chemical processes in the CFD simulations.

Photocatalytic materials promotes the reduction of pollutant concentrations via deposition. NO removal due to photocatalytic materials is modelled as a sink of NO concentration on the photoactive surface. The deposition flux of NO (F_{dep}) is modelled depending on the NO concentration close to the surface and the characteristic deposition velocity (V_d) of each photocatalytic material: F_{dep}= - NO $\cdot$ V_d. The deposition velocity (V_d) stands for the NO rate adsorbed by the photoactive surface, which is representative of the efficiency of each material to remove NO concentration in the air. Several studies tackled the computation of deposition velocities for photocatalytic materials using different approximations (Engel et al., 2015; Palacios et al., 2015a; Ifang et al., 2014). The deposition velocity for NO is computed based on the inlet and outlet concentrations in the photo-reactor under laboratory conditions (ISO 22197-1:2007). These standard conditions allow to quantify the efficiency of photocatalytic materials just using NO concentration at inlet. Hence the deposition velocity can only be estimated for NO. In the case of NO_2, its reduction is tackled by modelling atmospheric chemical reactions. TiO_2 surface adsorbs NO molecules reducing the ambient concentration of NO. In this way, less NO is converted to NO_2 by means of the chemical reaction with O_3 ($NO + O_3 \rightarrow NO_2 + O_2$), which is involved in the photostationary state, and therefore, NO_2 concentration in air is reduced.

3. Modelling the deposition effect of a photocatalytic material

This section aims to evaluate whether CFD simulations using the deposition velocity derived from laboratory tests are capable of reproducing the pollutant concentrations exposed to a photocatalytic material applied in an outdoor experiment.

3.1. Case description and simulation setup

Figure 1 depicts the computational domain (40 m x 40 m x 20 m) of a photocatalytic coating of around 700 m^2 spread over a flat terrain far away from traffic emissions. More details about the field campaign carried out in this experimental deployment can be found in Palacios et al. (2015a) and German et al. (2015). NO and NO_2 concentrations were recorded at several heights at 0.16, 0.85 and 2.7 m above ground level (L1, L2 and L3 respectively) in a measurement tower deployed in the centre of the coating. An additional sampling point is located out of the photoactive surface at 3.4 m height. At this site, used as a reference point for inlet conditions of the CFD simulations, concentrations of NO and NO_2, wind speed and direction, and temperature were measured. An irregular polyhedral mesh of around 115 000 grid points is used. Grid resolution is set to 0.5 m that gradually decreases in parallel cells to the ground to 0.4 m, 0.2 m and 0.08 m.

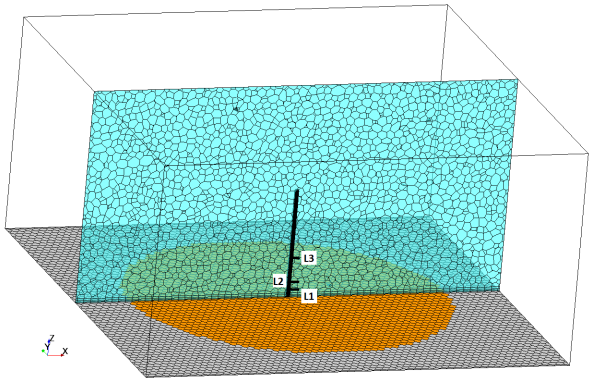

Figure 1: (a) Computational domain of the experimental deployment, where orange area stands for the photocatalytic coating.

Most favourable conditions to capture the maximum impact of photocatalytic materials were found from 1200 LST to 1400 LST on 29^{th} October 2014 (Palacios et al., 2015a). During these hours, meteorological conditions were nearly constant with wind speeds lower than 1.5 m s^{-1} and solar radiation higher than 400 W m^{-2}. Five scenarios are simulated every 30 min for that period up to reach the quasi-steady state at 1200 LST, 1230 LST, 1300 LST, 1330 LST and 1400 LST. Inlet meteorological variables are imposed assuming neutral atmospheric conditions for wind speed, turbulent kinetic energy and its dissipation rate as follows (Richards and Hoxey, 1993),

$$u_{in}(z) = \frac{u_*}{\kappa} ln\left(\frac{z}{z_0}\right) \quad k_{in} = \frac{{u_*}^2}{{C_\mu}^{1/2}} \quad \varepsilon_{in}(z) = \frac{{C_\mu}^{3/4} {k_{in}}^{3/2}}{\kappa z} \tag{4}$$

where κ is the von Karman constant (0.4), z_0 the roughness length (0.001 m), and u_* the friction velocity, which is computed from the measured wind speed (around 1 m s^{-1} at the reference point).

The measured air temperature (T_{air}) is about 294 K, which is established through a homogeneous profile at inlet of the CFD simulations. Additionally, the temperature of photocatalytic surface ($T_{coating}$) is imposed in the coating (orange area in Fig. 1) based on the measurements collected during the field campaign ($T_{coating}$=304 K). Hence buoyancy effects are also simulated based on the Boussinesq approximation with the CFD model (Santiago et al., 2014).

Inlet pollutant concentrations, NO and NO_2, are obtained from measurements at the reference point and are uniformly distributed at inlet boundary. The study area is located far away from any perturbation of traffic emissions. Hence the photochemical equilibrium is properly assumed to compute the inlet O_3 concentration by means of O_3=J_{NO_2}·NO_2 /k· NO, where chemical constants k and J_{NO_2} are computed depending on air temperature and zenith angle respectively (Finlayson-Pitts and Pitts Jr, 1999). Table 1 involves the inlet concentrations of NO, NO_2 and O_3 imposed in the simulations at each time.

Table 1: Inlet concentrations for each scenario (in ppb).

	1200 LST	**1230 LST**	**1300 LST**	**1330 LST**	**1400 LST**
NO (ppb)	15.04	23.74	22.29	15.10	9.52
NO_2 (ppb)	24.49	32.25	32.19	28.57	23.60
O_3 (ppb)	26.68	22.08	22.91	28.76	35.25

Lastly, NO deposition over the photocatalytic coating is modelled using the deposition velocity calculated for the material applied in this scenario, V_d=4.72 · 10^{-3} m s^{-1} (Palacios et al., 2015a).

3.2. Evaluation of modelling results with measurements

a. Assessment of the deposition velocity

The value used for the deposition velocity to simulate the NO removal is evaluated with measurements collected at the experimental system (Fig. 1). To do that, several CFD simulations are performed with no deposition and assuming a range of deposition velocities around the estimated value: V_d (=4.72 10^{-3} m s^{-1}), $0.1V_d$ (=4.72 10^{-4} m s^{-1}), $0.5V_d$ (=2.36 10^{-3} m s^{-1}), $2V_d$ (=9,44 10^{-3} m s^{-1}) and $10V_d$ (=4.72 10^{-2} m s^{-1}).

Figure 2a displays the measured NO at L1, and the NO simulated with no deposition and accounting for the range of V_d. The model results reveal that just a significant variation of V_d (NO[$10V_d$]) provides a noticeable reduction of the modelled NO in the air. The small differences in the modelled NO from the rest of the cases hinder the selection of the best approximation to the observations. Hence the relative difference of NO between L2 and L1 (computed as (NO_{L_2}−NO_{L_1})/NO_{L_1} × 100) are also assessed to determine the appropriate deposition velocity required to simulate the photocatalytic effect in real atmospheric conditions (Fig. 2b). The statistics (NMSE, FB, and MAE) are computed for each case based

on the observed and modelled vertical gradient of NO (ΔNO = NO_{L_2}−NO_{L_1}) at the lowest levels (Table 2).

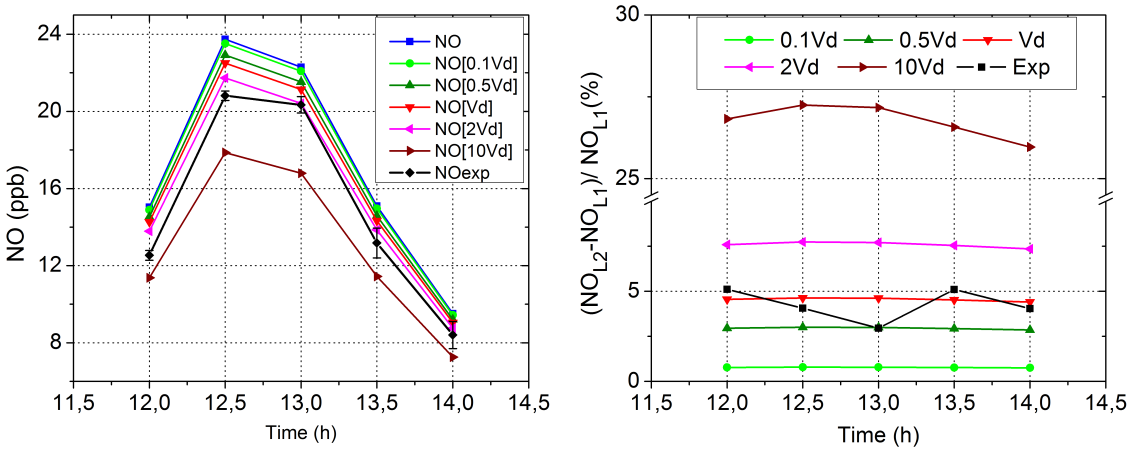

(a) **(b)**

Figure 2: (a) Measured NO concentration (NOexp) and NO simulated with no deposition (NO) and with the range of velocities: V_d (NO[Vd]), $0.1V_d$ (NO[0.1Vd]), $0.5V_d$ (NO[0.5Vd]), $2V_d$ (NO[2Vd]), $10V_d$ (NO[10Vd]). (b) Relative differences of NO between L2 and L1 for the experimental case (Exp) and the simulated cases: Vd, 0.1Vd, 0.5Vd, 2Vd and 10Vd.

Under the same atmospheric conditions, the only difference between one case and another is the efficiency to remove NO through the magnitude of deposition velocity. The vertical percentage reduction of NO using V_d and $0.5V_d$ exhibits similar values to that obtained from the observations (Fig. 2b). Based on the metrics for ΔNO, NO[$0.5V_d$] tends to underestimate the NO reduction (FB= -0.23 in Table 2). However, the simulated NO with V_d (=4.72 10^{-3} m s^{-1}), NO[V_d], yields slightly closer results of ΔNO to the observations (FB=0.18 and MAE=0.06 ppb). Therefore, the implementation of the deposition velocity, derived from the laboratory tests, provides an accurate modelling approach to reproduce the impact of the photoactive surfaces on ambient pollutants. It is worth pointing out that this modelling approach has been tested accounting for favourable meteorological conditions to observe the maximum activity of these materials.

Table 2: Model statistics for ΔNO.

	no V_d	**0.1**V_d	**0.5**V_d	V_d	**2**V_d	**10**V_d
NMSE	> 4	2.9	0.08	0.07	0.52	3.97
FB	-2.00	-1.30	-0.23	0.18	0.64	1.40
MAE [ppb]	0.34	0.27	0.08	0.06	0.30	1.55

b. Assessment of NO_2 concentration

The NO_2 concentration for the case NO[V_d] is also compared against measurements to ascertain that the resulting reduction of NO_2 is accurately reproduced by the chemical reactions. Both the modelled and measured NO_2 barely vary in height as a consequence of the large vertical mixing (Fig. 3). Hence the difficulty to observe a significant removal of NO_2 due to the photoactive surface.

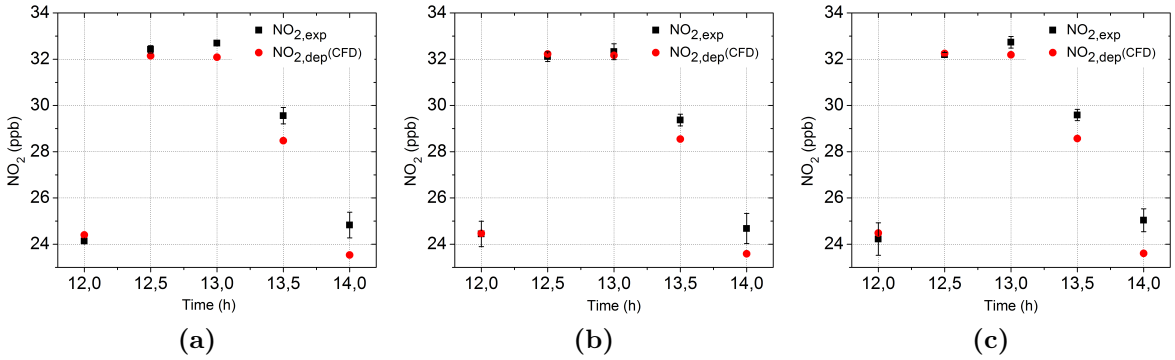

Figure 3: Modelled NO_2 for the case NO[V_d] ($NO_{2,dep}$ (CFD)) and measured NO_2 ($NO_{2,exp}$) at (a) L1, (b) L2 and (c) L3.

To examine the photocatalytic effect on NO_2, the vertical variation of NO_2 is computed for the simulations without NO deposition (NO) and with V_d (NO[V_d]). The observed NO_2 at the lowest levels presents a large fluctuation between negative and positive vertical gradients, which prevent an appropriate statistical comparison between the model and observations. A more stable behaviour for the NO_2 is observed between the L1 and L3 with an overall relative reduction of about 0.35%. Such gradient from the simulation without NO deposition is practically nonexistent ($\approx 10^{-5}$). However, a deviation of NO_2 of about 0.32% is captured by the model for the simulation with NO[V_d]. Despite the small reduction obtained for NO_2, the implementation of the chemical scheme allows to capture the impact on NO_2 as a result of the NO deposition on the photocatalytic coating.

Once the modelling approach to simulate the effect of photocatalytic materials is properly evaluated in outdoor conditions, this methodology is also applied to study the impact of these materials on air pollution in urban environments. The following sections are addressed to analyse the effect on NO_2 in air after applying photocatalytic materials on an real urban area using CFD simulations. Section 4 describes the area of interest and simulation setups for each studied case. Results and discussion are explained in Section 5.

4. Application of photocatalytic materials in an urban area

First, the study area, measurements sites and the computational domain are described in Section 4.1. Section 4.2 presents the setup of simulations performed on: a real case and an

hypothetical case. In the real case, modelled concentrations of NO and NO_2 are compared against measurements taken during the field campaign (Section 4.3).

4.1. Study area and CFD domain

The area of interest is located in Alcobendas, close to Madrid (Spain). In this location, an area of about 1000 m^2 was covered with photocatalytic material on the road of one of the main streets, where an intensive field campaign was carried out within the framework of the LIFE MINOx-STREET project (more details in Part I (Fernández-Pampillón et al., 2020)). Six sampling points were deployed along the study street collecting concentrations of NO and NO_2 at 0.4 m height (blue dots in Fig. 4). In addition, a reference point is placed above a building's roof at approximately 16 m above ground level (green dot in Fig. 4a) recording background atmospheric conditions of the area of interest every 5 min (wind speed and direction, temperature and air composition).

Figure 4a shows the buildings layout of the study area on the flat computational domain. The domain size is around 1500 m x 1000 m x 160 m, where the mean height of buildings is about 16 m and tallest building reaches around 20 m height. Based on the building footprints provided by the Alcobendas City Council, the buildings height are estimated using Google Earth images. The dimensions of the domain are established following the best practise guideline (Franke et al., 2007). A polyhedral mesh of $2.3 \cdot 10^6$ grid points is used with a grid resolution that gradually decreases from 6 m at the boundaries to 2 m in the research area (black square in Fig. 4a), and finer resolution is employed through parallel cells to the ground. Traffic emissions are imposed along main streets in CFD domain (red lines in Fig. 4a). The surface covered with photocatalytic material in the simulation is represented by the yellow area in Fig. 4.

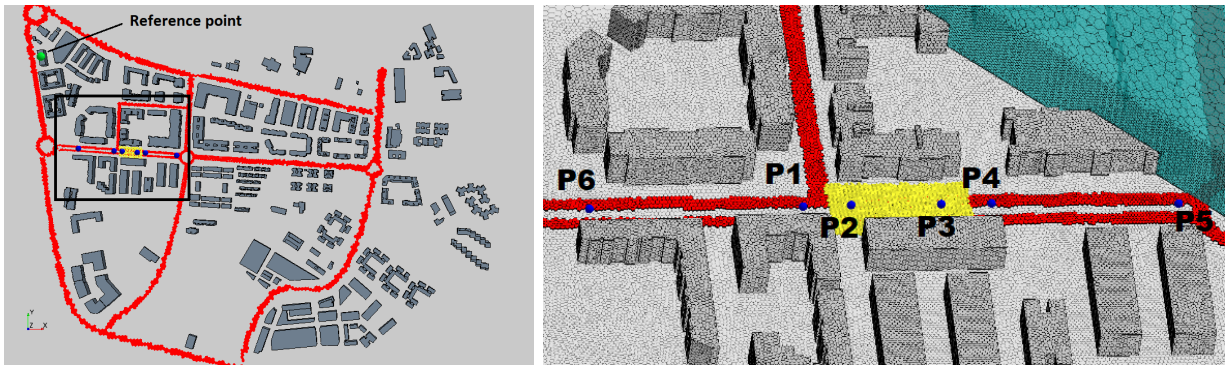

(a) **(b)**

Figure 4: (a) Computational domain of the selected urban area. (b) Irregular polyhedral mesh and measurement locations in the study street. Red lines represent location of traffic releases and yellow zone the area covered with photocatalytic material.

4.2. Simulation setup

a. Simulation setup of the real case

This simulation is performed from 1200 LST to 1300 LST on 29^{th} September 2015 in accordance to the study performed in Fernández-Pampillón et al. (2020). At that time, wind speed is low (around 3.4 m s^{-1} at the reference point) and besides, a large area of photoactive surface is sunlit, which promote to capture a greater impact of photocatalytic material on ambient pollutant at street level. The selection of that day is also due to the required inputs to undertake the simulation were all available from measurements collected during the field campaign (Fernández-Pampillón et al., 2020).

The CFD simulation is performed in unsteady conditions using 1-s timestep for both dynamical processes and chemical reactions of the photostationary state. All data required to initialize the CFD simulation are derived from the reference point and thus, boundary conditions change every 5 min. Meteorological conditions are established in neutral atmospheric conditions (Eq. 4) where wind blows from South-East. Inlet concentrations of NO, NO_2 and O_3 vary over time around 5-7 ppb, 9-12 ppb and 39-47 ppb respectively.

Traffic-related emissions of NO and NO_2 are computed accounting for traffic flow recorded with a camera in the study street (Fernández-Pampillón et al., 2020). For that, the number of vehicles are clustered every 5 min being almost 700 veh per hour, from 1200 LST to 1300 LST. Therefore, traffic emissions are uniformly imposed on each street and are changing every 5 min. The emitted NO_x are estimated depending on emission factors for each kind of vehicle whereof ratio NO_2/NO_x is assumed to be 0.3 (Borge et al., 2014). For the rest of streets in the domain, traffic emissions are estimated based on the annual daily traffic flow reported by Alcobendas City Council (Alcobendas-Council, 2005), keeping the traffic flow ratio between each street and the study street at 1200 LST.

NO deposition over the photoactive area is modelled through a surface flux (F_{dep} = -NO·V_d). The photocatalytic material implemented over the pavement provided a NO removal efficiency of around 46% in laboratory conditions. Distinct approximations are developed to compute the V_d for photocatalytic materials. However, the small variation in the magnitude of V_d resulted in a similar reduction of the modelled NO in the air (Sanchez et al., 2015). For consistency with the method followed in Section 3, the deposition velocity used for NO was estimated through the mass-balance approximation with laboratory data, and its value was V_d=$5.25 \cdot 10^{-3}$ m s^{-1} (Palacios et al., 2015a).

b. Simulation setup of the hypothetical case

This additional case is addressed to assess the effect of photocatalytic materials by expanding photoactive surface to an entire neighbourhood covering an area of about 0.98 km^2. In this hypothetical case, roads, walls and sidewalks are modelled as photoactive surfaces (orange shades in Fig. 5). During the LIFE MINOx-STREET Project, multiple photocatalytic materials were tested according to the type of urban surface i.e. asphalt pavement, facades or sidewalks (Palacios et al., 2015a,b). Apart from the photocatalytic material used for the

road, two additional materials specific for facades and sidewalk were also examined in the project. Hence different deposition velocities are employed in this section depending on the type of urban surface (Table 3).

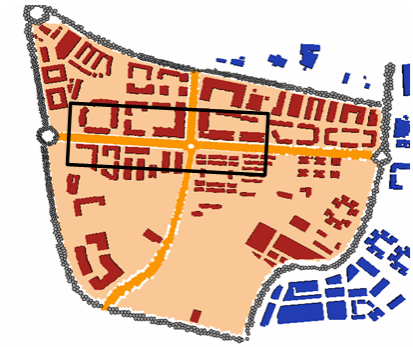

Figure 5: Photoactive area at neighbourhood scale. Note that different orange shades stand for different V_d, representative of each photocatalytic material prepared for road, walls and sidewalks.

Table 3: Deposition velocities of NO for each surface: road, sidewalk and wall (Palacios et al., 2015a,b).

Deposition velocities	$m\ s^{-1}$
Road	$5.25\ 10^{-3}$
Sidewalk	$10.1\ 10^{-3}$
Wall	$3.57\ 10^{-3}$

The main assumption is that all photoactive surfaces are completely sunlit and acting as its maximum efficiency. Despite the fact that it is not realistic, this study is performed to seek the highest effect of applying photocatalytic materials over a bigger area on the NO_2 reduction in air within the area of interest.

Simulations are undertaken focusing on prevailing atmospheric conditions at 1200 LST recorded from November 2014 to January 2015 in the research area. Hence inlet values for wind speed and direction, temperature and pollutant concentrations are obtained from hourly values averaged at that time over 3 months. With prevailing wind direction from SE, neutral atmospheric stability is assumed for inlet profile of wind speed and turbulent parameters (Eq. 4). Inlet concentrations of NO, NO_2 and O_3 are set at 21 ppb, 17 ppb and 22 ppb. The photostationary state is considered to model chemical conversions and hence simulations are performed using 1 s timestep up to reach the quasi-steady state.

Additionally, the variability of wind speed and traffic emissions in urban environments is also assessed in order to determine how the NO_2 reduction is affected. Based on the information collected in the study street (reference case), two wind speed scenarios (3.4 m s^{-1} (reference

case) and 1.7 m s^{-1} at 10 m) and four traffic emissions (EmSc (reference case), 4×EmSc, 8×EmSc and 12×EmSc) are considered. Traffic emissions of NO_x for EmSc are computed assuming the number of vehicles in the actual case multiplied by an average NO_x emission factor per vehicle (=0.5 g km^{-1}) (HBEFA, 2010).

4.3. Evaluation with measurements in the real case

In this section, dispersion of pollutants in the real case is evaluated with experimental data taken at the sampling points in the street (P1 to P6 in Fig. 4b). Due to the proximity of measurements to traffic emissions, strong variability of observations is not completely reproduced by the model since emissions of each individual vehicle are not explicitly modelled by the CFD simulation. Therefore, for an adequate comparison with observations, both measured and modelled concentrations of NO and NO_2 at the sampling points are averaged over the entire hour (Fig. 6).

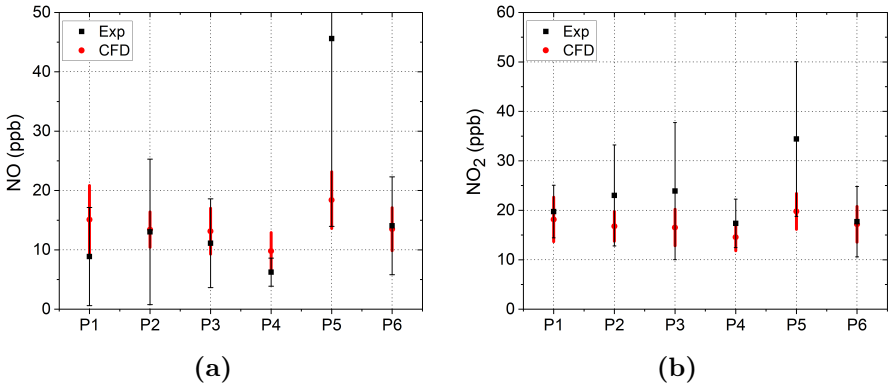

Figure 6: Averaged concentrations and standard deviations obtained from measurements (Exp) and simulation (CFD) at sampling points for: (a) NO (ppb) and (b) NO_2 (ppb).

Modelled concentrations of NO and NO_2 are within the variability range of observations at most of the points, though present an overall underestimation with FB= -0.171 and FB= -0.276 respectively. Additionally, the NMSE shows a general deviation for both NO and NO_2 with values NMSE=0.84 and NMSE=0.73 (NMSE<1.5 (Chang and Hanna, 2004)) respectively. The mean absolute error obtained for NO is 6.66 ppb, whereas for NO_2 is 5.50 ppb. This difference in concentration is clearly due to the underestimation in concentrations of NO and NO_2 at P5. At this point, standard deviations of measured concentrations reveal a great range of variability, which seems to be highly influenced by traffic emissions from the nearest roundabout. It is noteworthy that the uncertainties of the emissions in that roundabout are larger that in the study street because traffic flow information was not available there. Therefore, the underprediction of NO concentration at P5 seems to be caused by an underestimation of the emissions from the roundabout traffic flow. Despite the deviation obtained at P5, modelled concentrations of NO and NO_2 along the study street properly fit to the measured concentrations at the other sites.

5. Results

The complexity of dynamics, chemical and turbulent processes together with the multiple obstacles that exist in urban areas may hinder the observation of pollutants reduction in air because of the photocatalytic effect. Nevertheless, through CFD simulations, mitigation on NO_2 concentrations can be quantified by means of the difference between two simulations, with and without considering the deposition flux over the photoactive surface under the same atmospheric conditions. Hence NO_2 removal can be estimated by the following expression,

$$\delta NO_2(\%) = \frac{NO_{2,\mathrm{dep}} - NO_2}{NO_2} \cdot 100 \tag{5}$$

where $NO_{2,dep}$ and NO_2 are resulted from modelled NO_2 concentrations with and without considering NO deposition flux on the photocatalytic surface, respectively.

The reduction effect on urban air pollution by applying photocatalytic materials in urban environments has to be assessed at a representative height of population exposure. This height is established at 3 m above ground level, where monitoring stations used to assess air quality in cities record air pollutants levels. For that reason, in the following sections the reduction of pollutant concentrations due to photocatalytic materials is examined at 3 m in the research area.

5.1. Real Case

At 1300 LST, the modelled wind speed at 3 m barely reaches velocities of 1 m s^{-1} producing irregular circulations in the study street (Fig. 7a). The spatial distribution of NO and NO_2 show that the highest concentrations are mainly placed on the road near the traffic emissions (Fig. 7b-d). Figure 7c-e exhibits the NO removed by deposition on the photoactive surface (computed as $\delta NO(\%)=(NO_{dep}\text{-}NO)/NO \cdot 100$) and thus, the reduction of NO_2 (δNO_2) at 3 m height. Maps of δNO and δNO_2 highlight that the reduction of pollutants is mainly noticeable over the photoactive area and rapidly decreases in the wind flow direction. The largest differences are just obtained in the vortexes formed in the street. Lower wind speed increases the residence time of pollutants, and as a result, raises the probability of a molecule of NO interacts with the photoactive surface.

In this scenario, δNO varies from 1.8% to 3%, whereas the NO_2 reduction hardly reaches 1.1%. δNO_2 ranges between 0.4% and 1.1% exclusively over the photoactive surface. The maximum reductions, both for NO and NO_2, are limited to the nearest areas to the photoactive surface. Due to the 3-reactions mechanism used in the simulations, the decrease in the NO and NO_2 lead to a slightly increase of the O_3 at pedestrian level (not shown). Similar to NO and NO_2, the largest increase of O_3 is obtained close to the photoactive area, though its concentrations only enhance 0.6% as much. Additionally, the extent of its impact is in turn modulated by the wind flow pattern within the street, which can also be observed through the vertical profiles of δNO_2 at the sampling points at 1300 LST (Fig. 8).

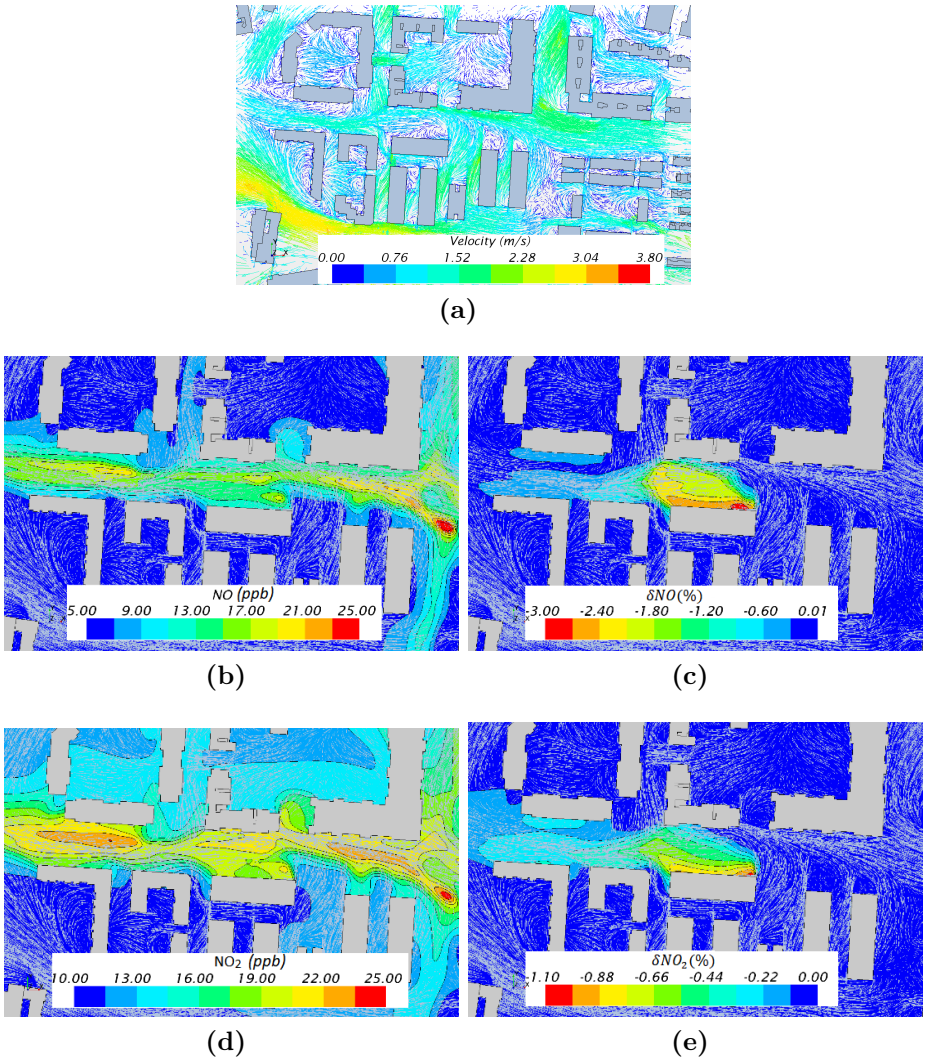

Figure 7: At 1300 LST, horizontal sections (z=3 m) of: (a) wind speed (m s^{-1}) (b) NO (ppb), (c) δNO (%), (d) NO_2 (ppb) and (e) δNO_2 (%).

Vertical profiles of δNO_2 at sampling points present maximum values over the photoactive surface (P2 and P3) that is rapidly reduced in height. However, different profile is obtained at P6, where δNO_2 takes maximum difference at 10 m height, though its value is rather low. This behaviour on NO_2 deviation is mainly caused by vertical mixing produced within the street and chemical conversions between NO and NO_2. Wind direction blows from east to west of the street dragging pollutants emitted from vehicles in that direction. Whereas there is no reduction in NO_2 concentrations at P5, δNO_2 increases by crossing the photoactive surface at P3 and reaches the highest value at P2. At P1 and P6, vertical mixing dilutes the effect of photocatalytic material raising the maximum values of δNO_2 in height, but its impact on NO_2 concentrations is reduced (δNO_2 <0.25% at P6). Therefore, the effect of NO deposition over a delimited photoactive area in the street can be noticed beyond the treated

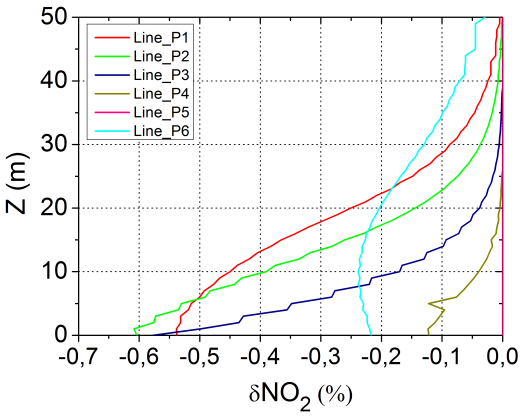

Figure 8: Vertical profiles at sampling points of δNO_2 (%) at 1300 LST.

surface, however mixing of pollutants from fresh emissions and background concentrations considerably reduce the impact on NO_2 levels. In addition, as airmass travels over a larger photocatalytic area, a greater reduction on NO_2 concentration is obtained.

5.2. Hypothetical case

Due to the minimal reduction of NO_2 obtained in the previous case, a broader study is carried out assuming a wider photoactive area (orange areas in Fig. 5). Additionally, a sensitivity test is performed to better understand how the variations in wind speed and traffic emissions can affect the NO_2 removal caused by photocatalytic materials (Table 4). It is worth pointing out that the model results presented in this section are based on the prevailing atmospheric conditions for the research area at 1200 LST (Case 1_{high}).

Table 4: Simulated cases considered for the sensitivity test.

Traffic Emission \ wind speed	$U_{z=10m}$=3.4 m s^{-1}	$U_{z=10m}$=1.7 m s^{-1}
EmSc	Case 1_{high}	Case 1_{low}
4×EmSc	Case 2_{high}	Case 2_{low}
8×EmSc	Case 3_{high}	Case 3_{low}
12×EmSc	Case 4_{high}	Case 4_{low}

Figure 9 displays the wind flow pattern and the spatial distribution at 3 m height of NO_2, $NO_{2,dep}-NO_2$ and δNO_2 for the Case 4_{low} and Case 4_{high}. Wind flow blows from south-east with an average velocity in the street of about 1.22 m s^{-1} in the Case 4_{high} and 0.61 m s^{-1} in the Case 4_{low}. Hence the average NO_2 in the street increases from 45 ppb to almost 70 ppb with the lower wind speed (Fig. 9c-d). For both cases, δNO_2 hardly reaches 3% on the road with an average reduction of 1.1% in Case 4_{high} and 1.5% in Case 4_{low}. In addition, the spatial distribution of $NO_{2,dep}-NO_2$ shows a minimal removal below 1.2 ppb on the road.

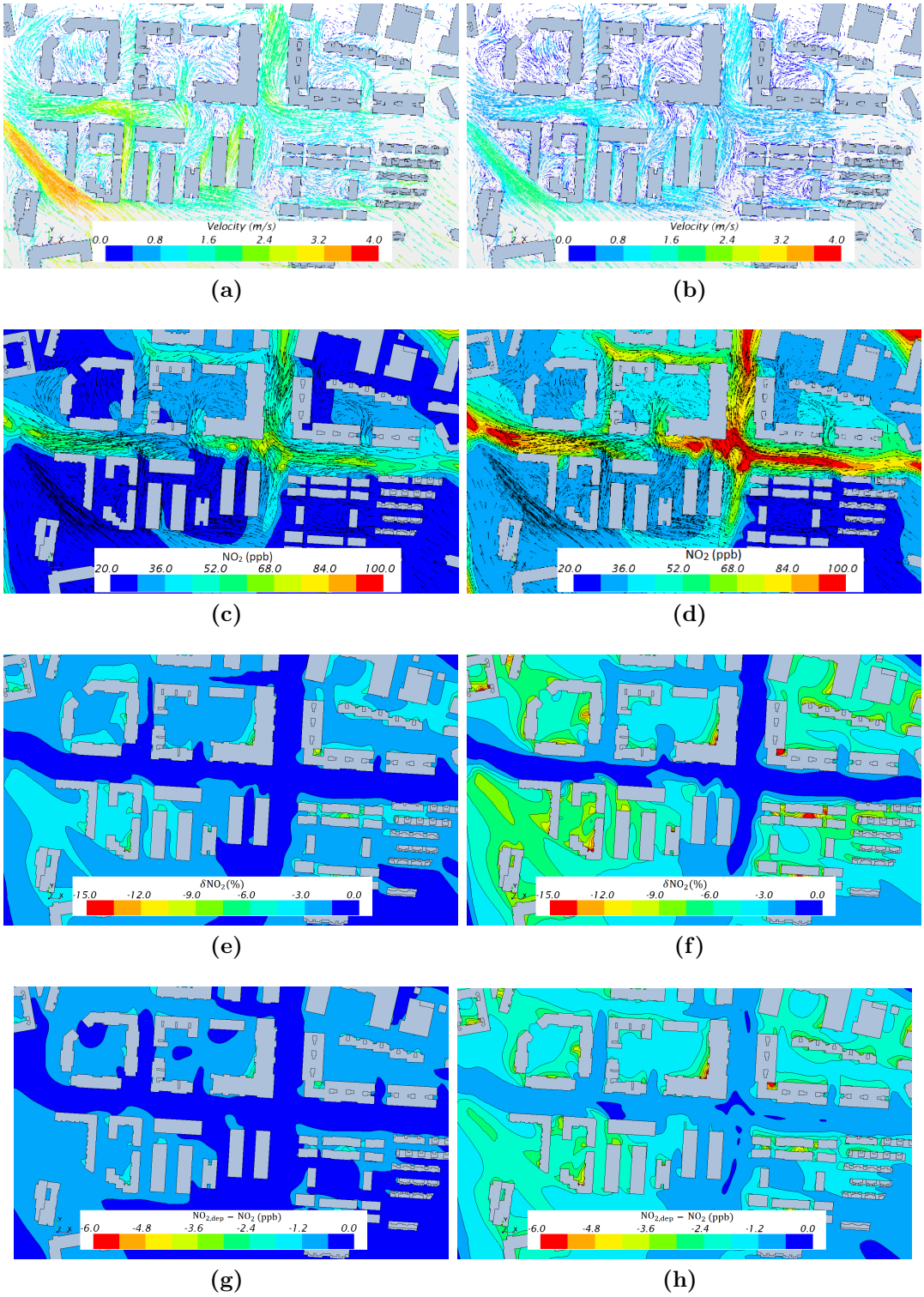

Figure 9: Horizontal section (z=3 m) of: (a) wind speed (m s^{-1}), (c) NO_2 (ppb), (e) δNO_2 (%) and (g) $NO_{2,dep}-NO_2$ (ppb) for Case 4_{high}. Same as Case 4_{high}, but for Case 4_{low} in (b), (d), (f) and (h) respectively.

In the surrounding areas to the road zone, δNO_2 yields larger values (above 3%) in far areas away from traffic emissions, where the NO_2 concentration is generally lower. Nonetheless, the $NO_{2,dep}$ differs as much 1.2 ppb from 20 ppb of NO_2 in the Case 4_{high} and around 3 ppb over 30 ppb in the Case 4_{low}. It is worth noting that all the urban surfaces are considered simultaneously photoactive. Such difference is due to the high contribution of the NO_x emission to the ambient pollutants on the road, which minimizes the impact of the deposition process. Therefore, the latter becomes more relevant in areas less affected by the traffic emissions and thus, with lower NO_2.

Focusing on the road, where the highest levels of NO_2 are found and the pedestrian exposure is also higher, the spatial average of δNO_2 and NO_2 ($<NO_2>$) in the street zone are assessed at 3 m height for all simulated cases in Table 4 (Fig. 10).

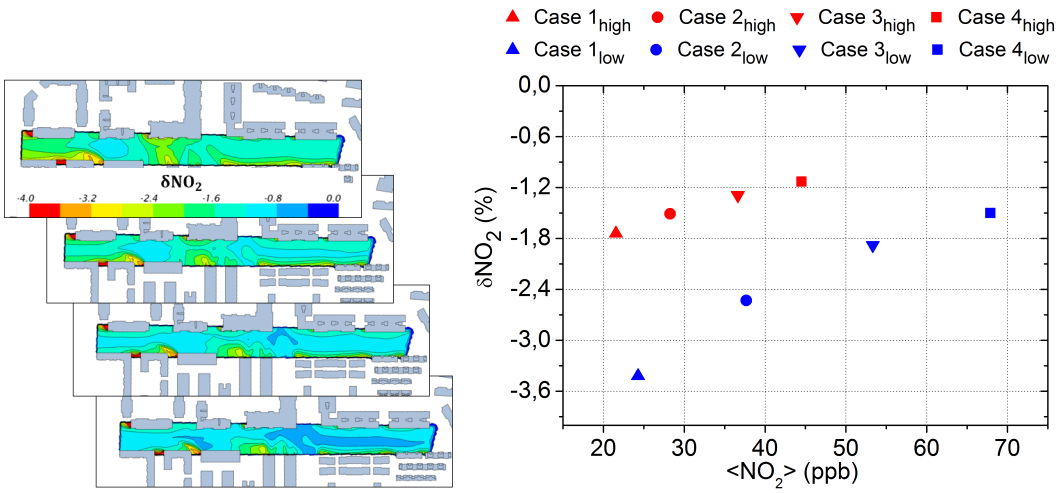

Figure 10: (a) (top to bottom) δNO_2 map (z=3 m) for the Case 1_{high} to Case 4_{high} in %. (b) Plot of spatial average in the street (z=3 m) of δNO_2 against that the NO_2 concentration ($<NO_2>$) for all cases involved in Table 4.

For the two distinct wind regimes, the average NO_2 removal decreases by increasing the NO_2 concentration in the street, mainly because of the NO_x emissions increase. Therefore, the relative contribution to the ambient NO_2 due to the emission rate is greater than the deposition rate, which diminish the impact of the NO deposition on the NO_2 levels. Spatial average of δNO_2 ranges from 3.42% to 1.50% with lower wind speed, however, it hardly varies around 1.5% with higher wind speed. Lower velocities promote the reduction of NO_2 since the residence time of pollutants in the street increases. Apart from the influence of wind speed, the NO_2 reduction might varies according to the traffic emission scenario. Whereas the average δNO_2 goes up from 1.72% for the Case 1_{high} to 3.42% for the Case 1_{low} raising as wind speed decreases, δNO_2 barely increases from 1.1% in Case 4_{high} to 1.5% in Case 4_{low} in a heavy traffic emissions scenario.

6. Conclusions

This work aims at assessing the potential of photocatalytic materials applied in urban environments to reduce NO_2 concentrations at pedestrian level through CFD simulations. The model performance is evaluated with measurements collected in different field campaigns. In the experimental system, the impact of photocatalytic material on NO_x ambient concentrations is properly modelled by means of a deposition velocity for NO computed from laboratory data. Hence the implementation of a chemical mechanism is required to reproduce the NO_2 reduction after NO is deposited on the photoactive area. Likewise, the comparison of the modelled NO_2 concentration using the photostationary state lead to a successful approximation of the observed NO_2 concentrations.

Additionally, NO_2 reduction is quantified and analysed under multiple atmospheric conditions in a real urban setting. In these simulations, turbulence induced by vehicles and thermal effects caused by heating of urban surfaces are not considered, which would increase the turbulent mixing of pollutants in the street. Despite these limitations, the CFD simulations are capable of reproducing the NO_2 concentrations in a real street. Two cases are addressed to study the NO_2 reduction due to photocatalytic materials in an urban area: (a) a real case, where an area of around 1000 m^2 is treated with photocatalytic material, and (b) an hypothetical case, where a no realistic area of about 0.98 km^2 is considered assuming all urban surfaces are simultaneously photoactive. In the latter, the influence on the NO_2 reduction caused by the variability of wind speed and traffic intensity is examined.

Modelling results improve the understanding of the impact of applying photocatalytic materials in urban environments on ambient NO_2 at pedestrian level, and the following conclusions are drawn:

- In the real case, the application of the photocatalytic material provides a minimal reduction (below 1%) for NO_2 concentration and a maximum of 3% for NO at pedestrian level under the studied atmospheric conditions. Maximum values are reached in specific areas modulated by the wind flow pattern in the street and this reduction rapidly decrease with height.

- Increasing the photoactive surfaces in the hypothetical case, the mean NO_2 reduction in the street ranges between 1.8% (high wind case) and 3.4% (low wind case). This is because wind flow modulates the residence time of pollutants in the street affecting the NO deposition. Therefore, lower (higher) wind speed increases (decreases) the deposited NO on the photoactive surface and thus, the percentage reduction of NO_2 air is higher (lower).

- An increase of NO_x emissions lead to an increase of the NO_2 concentrations in the street, however the percentage reduction of NO_2 tends to decrease up to 1.4% (low wind case) and 1.2% (high wind case) in the highest emissions scenario. This indicates that the emission rate is larger than NO deposition rate and chemical conversion to NO_2. This trend reveals that the impact of photocatalytic materials on NO_2 levels becomes smaller in highly polluted areas, such as urban hot-spots.

It is worthwhile pointing out that numerical values of pollutants removal derived from the hypothetical case should be considered as an upper limit. In addition to the application of photocatalytic materials to all urban surfaces is not feasible, in real-world conditions, the surfaces are not simultaneously sunlit due to the shadows produced by the urban morphology. Hence the fact that all urban surfaces cannot be photoactive at the same time. Accordingly, this percentage reduction will be significantly lower in real atmospheric conditions, in particular, when the peaks of NO_2 occur in the early morning or in the evening since most of the surfaces are shaded.

This work focuses on a specific urban area based on prevailing meteorological conditions recorded in this neighbourhood (at 1200 LST). Accordingly, values of δNO_2 can vary from this urban area to another due to differences in geometry and layout of buildings, meteorological conditions or local traffic emissions. For instance, a denser urban area with taller buildings and narrower streets would increase the residence time of NO and so its probability to be deposited. However, the shadowing would reduce the area of photoactive surfaces. Nevertheless, the overall trend obtained in this study about the capability of photocatalytic materials to mitigate NO and NO_2 at pedestrian height in a real-world environment and the influence of atmospheric conditions can be expected to be valid to any city.

Acknowledgments

This study has been supported by LIFE MINOx-STREET project (LIFE12 ENV/ES/000280) funded by European Commission. Authors thank to our collages involve in field campaigns for sharing all of experimental data used in this work to evaluate the CFD simulations. In addition, we are grateful to Alcobendas City Council for providing the footprints of buildings of the study area. Authors also thank to Extremadura Research Centre for Advanced Technologies (CETA-CIEMAT) for easing the use of its computational resources to carry out the simulations. CETA-CIEMAT belongs to CIEMAT and the Government of Spain and is funded by the European Regional Development Fund (ERDF).

References

Alcobendas-Council, 2005. Plan de movilidad urbana. Ayuntamiento de Alcobendas, Madrid (in Spanish). URL: website: http://www.alcobendas.org/recursos/doc/Urbanismoinfraestructura/Informesmedioambientales/13115900311201413103 8.pdf.

Amorim, J., Rodrigues, V., Tavares, R., Valente, J., Borrego, C., 2013. Cfd modelling of the aerodynamic effect of trees on urban air pollution dispersion. Science of the Total Environment 461, 541–551.

Ballari, M.M., Brouwers, H., 2013. Full scale demonstration of air-purifying pavement. Journal of hazardous materials 254, 406–414.

Ballari, M.M., Hunger, M., Hüsken, G., Brouwers, H., 2010. Modelling and experimental study of the nox photocatalytic degradation employing concrete pavement with titanium dioxide. Catalysis Today 151, 71–76.

Borge, R., Lumbreras, J., Pérez, J., de la Paz, D., Vedrenne, M., de Andrés, J.M., Rodríguez, M.E., 2014. Emission inventories and modeling requirements for the development of air quality plans. application to madrid (spain). Science of the Total Environment 466, 809–819.

Buccolieri, R., Santiago, J.L., Rivas, E., Sanchez, B., 2018. Review on urban tree modelling in cfd simulations: Aerodynamic, deposition and thermal effects. Urban Forestry & Urban Greening 31, 212–220.

Chang, J.C., Hanna, S.R., 2004. Air quality model performance evaluation. Meteorology and Atmospheric Physics 87, 167–196.

Chen, M., Chu, J.W., 2011. Nox photocatalytic degradation on active concrete road surface—from experiment to real-scale application. Journal of Cleaner Production 19, 1266–1272.

Clapp, L.J., Jenkin, M.E., 2001. Analysis of the relationship between ambient levels of o3, no2 and no as a function of nox in the uk. Atmospheric Environment 35, 6391–6405.

Cordero, J., Hingorani, R., Jimenez-Relinque, E., Grande, M., Borge, R., Narros, A., Castellote, M., 2020. Nox removal efficiency of urban photocatalytic pavements at pilot scale. Science of The Total Environment , 137459.

EEA, E.E.A., 2015. Air quality in europe – 2015 report. eea report no 5/2015. eea, copenhagen, denmark, p 57. http://dx.doi.org/10.2800/62459. Available online at: http://www.eea.europa.eu//publications/air-quality-in-europe-2015. 46, 145–153.

Engel, A., Glyk, A., Hülsewig, A., Große, J., Dillert, R., Bahnemann, D.W., 2015. Determination of the photocatalytic deposition velocity. Chemical Engineering Journal 261, 88–94. URL: http://dx.doi.org/10.1016/j.cej.2014.03.040, doi:10.1016/j.cej.2014.03.040.

Fernández-Pampillón, J., Palacios, M., Núñez, L., Pujadas, M., Sanchez, B., Santiago, J., Martilli, A., 2020. Nox depolluting performance of photocatalytic materials in an urban area - part i: Monitoring ambient impact. Atmospheric environment (submitted).

Finlayson-Pitts, B.J., Pitts Jr, J.N., 1999. Chemistry of the upper and lower atmosphere: theory, experiments, and applications. Elsevier.

Franke, J., Hellsten, A., Schlünzen, H., Carissimo, B., 2007. Best practice guideline for the CFD simulation of flows in the urban environment. COST Office Brussels.

Gallus, M., Akylas, V., Barmpas, F., Beeldens, A., Boonen, E., Boréave, A., Cazaunau, M., Chen, H., Daële, V., Doussin, J., et al., 2015a. Photocatalytic de-pollution in the leopold ii tunnel in brussels: Nox abatement results. Building and Environment 84, 125–133.

Gallus, M., Ciuraru, R., Mothes, F., Akylas, V., Barmpas, F., Beeldens, A., Bernard, F., Boonen, E., Boréave, A., Cazaunau, M., et al., 2015b. Photocatalytic abatement results from a model street canyon. Environmental Science and Pollution Research 22, 18185–18196.

German, M., Palacios, M., Pujadas, M., Nunez, Fernandez-Pampillon, J., 2015. Experimental study of nox depolluting capabilities of a photocatalytic coating tested under sub-urban ambient conditions, 12th Urban Environment Symposium. Oslo, Noruega. URL: http://www.lifeminoxstreet.com/life/showFile/242dc51b-f5a8-483b-a9e8-846f531ebe7a/?idioma=2.

Guerrini, G.L., 2012. Photocatalytic performances in a city tunnel in rome: Nox monitoring results. Construction and Building Materials 27, 165–175.

Hassan, M., Mohammad, L.N., Asadi, S., Dylla, H., Cooper III, S., 2012. Sustainable photocatalytic asphalt pavements for mitigation of nitrogen oxide and sulfur dioxide vehicle emissions. Journal of Materials in Civil Engineering 25, 365–371.

HBEFA, 2010. Handbook Emission Factors for Road Transport. Technical Report. Tech. rep., INFRAS, HBEFA 3.1. URL: Available online at: http://www.eea.europa.eu//publications/air-quality-in-europe-2017.

Hüsken, G., Hunger, M., Brouwers, H., 2009. Experimental study of photocatalytic concrete products for air purification. Building and environment 44, 2463–2474.

Ifang, S., Gallus, M., Liedtke, S., Kurtenbach, R., Wiesen, P., Kleffmann, J., 2014. Standardization methods for testing photo-catalytic air remediation materials: Problems and solution. Atmospheric Environment 91, 154–161. URL: http://dx.doi.org/10.1016/j.atmosenv.2014.04.001, doi:10.1016/j.atmosenv.2014.04.001.

Jeanjean, A.P.R., Gallagher, J., Monks, P.S., Leigh, R., 2017. Ranking current and prospective no2 pollution mitigation strategies: An environmental and economic modelling investigation in oxford street, london. Environmental Pollution 225, 587–597.

Jõgi, I., Erme, K., Raud, J., Laan, M., 2016. Oxidation of no by ozone in the presence of tio2 catalyst. Fuel 173, 45–51.

Kwak, K.H., Baik, J.J., Ryu, Y.H., Lee, S.H., 2015. Urban air quality simulation in a high-rise building area using a cfd model coupled with mesoscale meteorological and chemistry-transport models. Atmospheric Environment 100, 167–177.

Kwak, K.H., Woo, S.H., Kim, K.H., Lee, S.B., Bae, G.N., Ma, Y.I., Sunwoo, Y., Baik, J.J., 2018. On-road air quality associated with traffic composition and street-canyon ventilation: Mobile monitoring and cfd modeling. Atmosphere 9, 92.

Maggos, T., Plassais, A., Bartzis, J., Vasilakos, C., Moussiopoulos, N., Bonafous, L., 2008. Photocatalytic degradation of nox in a pilot street canyon configuration using tio 2-mortar panels. Environmental monitoring and assessment 136, 35–44.

Palacios, M., Núñez, L., Pujadas, M., Fernández-Pampillón, J., Germán, M., Sánchez, B., Santiago, J., Martilli, A., Suárez, S., Cabrero, B., 2015a. Estimation of no x deposition velocities for selected commercial photocatalytic products. WIT Transactions on The Built Environment 168, 729–740.

Palacios, M., Suarez, S., Nuñez, L., Sanchez, B., Pujadas, M., Fernandez-Pampillon, J., 2015b. Influence of parameters on the photocatalytic oxidation of nitric oxide at the surface of titanium dioxide-modified concrete materials, International Conference on Chemical and Biochemical Engineering. Paris, France. URL: http://www.lifeminoxstreet.com/life/showFile/56c895a5-6bd9-4c4c-b319-b96a6d01d9cc/?idioma=2.

Richards, P., Hoxey, R., 1993. Appropriate boundary conditions for computational wind engineering models using the k-ε turbulence model. Journal of wind engineering and industrial aerodynamics 46, 145–153.

Rivas, E., Santiago, J.L., Lechón, Y., Martín, F., Ariño, A., Pons, J.J., Santamaría, J.M., 2019. Cfd modelling of air quality in pamplona city (spain): Assessment, stations spatial representativeness and health impacts valuation. Science of the Total Environment 649, 1362–1380.

Sanchez, B., Santiago, J., Martilli, A., Palacios, M., German, M., Pujadas, M., Nuñez, L., Fernandez-Pampillon, J., 2015. Modeling the macroscopic effect as nox sink of a photocatalytic surface under real outdoor conditions, 12th Urban Environment Symposium. Oslo, Norway. URL: http://www.lifeminoxstreet.com/life/showFile/f89a9f19-b5d8-498e-b48a-2ab6e149047a/.

Sanchez, B., Santiago, J.L., Martilli, A., Martin, F., Borge, R., Quaassdorff, C., de la Paz, D., 2017. Modelling nox concentrations through cfd-rans in an urban hot-spot using high resolution traffic emissions and meteorology from a mesoscale model. Atmospheric environment 163, 155–165.

Sanchez, B., Santiago, J.L., Martilli, A., Palacios, M., Kirchner, F., 2016. Cfd modeling of reactive pollutant dispersion in simplified urban configurations with different chemical mechanisms. Atmospheric Chemistry and Physics 16, 12143–12157.

Santiago, J., Borge, R., Martin, F., de la Paz, D., Martilli, A., Lumbreras, J., Sanchez, B., 2017. Evaluation of a cfd-based approach to estimate pollutant distribution within a real urban canopy by means of passive samplers. Science of the Total Environment 576, 46–58.

Santiago, J., Borge, R., Sanchez, B., Quaassdorff, C., de la Paz, D., Martilli, A., Rivas, E., Martín, F., 2020. Estimates of pedestrian exposure to atmospheric pollution using high-resolution modelling in a real traffic hot-spot. Science of The Total Environment , 142475.

Santiago, J., Krayenhoff, E., Martilli, A., 2014. Flow simulations for simplified urban configurations with microscale distributions of surface thermal forcing. Urban climate 9, 115–133.

Schneider, J., Matsuoka, M., Takeuchi, M., Zhang, J., Horiuchi, Y., Anpo, M., Bahnemann, D.W., 2014. Understanding TiO 2 Photocatalysis: Mechanisms and Materials . Chemical Reviews 114, 9919–9986. doi:10.1021/cr5001892.

Seinfeld, J.H., Pandis, S.N., 1998. Atmospheric chemistry and physics: from air pollution to climate change. John Wiley & Sons.

WHO, 2013. Review of Evidence on Health Aspects of Air PollutioneREVIHAAP Project. Technical Report. World Health Organisation.

Zhong, J., Cai, X.M., Bloss, W.J., 2016. Coupling dynamics and chemistry in the air pollution modelling of street canyons: A review. Environmental Pollution 214, 690–704.

Zhong, J., Cai, X.M., Bloss, W.J., 2017. Large eddy simulation of reactive pollutants in a deep urban street

canyon: Coupling dynamics with o3-nox-voc chemistry. Environmental Pollution 224, 171–184.
Zouzelka, R., Rathousky, J., 2017. Photocatalytic abatement of nox pollutants in the air using commercial functional coating with porous morphology. Applied Catalysis B: Environmental 217, 466–476.